MEMS Pressure Sensor for High-Temperature Applications

Qiubin Zhao, Xingguo Xiong
Department of Electrical and Computer Engineering,
University of Bridgeport, Bridgeport, CT 06604

Abstract

MEMS pressure sensors have been widely used in automobiles, airplanes, submarines, and biomedical devices. For some special applications such as aerospace and underground oil exploration, pressure sensors which can endure extremely high temperature are required. In this paper, the design and simulation of a novel silicon-carbide based MEMS pressure sensor for high-temperature applications is proposed. The proposed MEMS pressure sensor is based on Si-SiC-Si compound structure. A SiC round plate supported by four flexible folded beams is sealed inside a vacuum cavity between the top silicon diaphragm and bottom silicon substrate. The gold electrodes deposited on SiC plate constitute top and bottom capacitances with top Si diaphragm and bottom Si substrate. When no external pressure is applied, the SiC round plate stays in the middle of the gap, and top capacitance equals to bottom capacitance. When an external pressure is applied, the top Si diaphragm deforms, and a DC driving voltage is applied between SiC plate and substrate to pull the SiC plate down to the middle position of the gap. In this way, the top capacitance is kept equal to the bottom capacitance. By measuring the required driving voltage, the applied external pressure is derived. This is the working principle of the SiC MEMS pressure sensor. The device model is analyzed in details, and a set of optimized design parameters of the device is derived. ANSYS FEM simulation is used to verify the vibration modes of the SiC plate. The proposed novel MEMS pressure sensor can be used for pressure sensing in high-temperature applications.

I. Introduction

Pressure measurement is needed in many industry applications, such as pressure monitoring in oil storage tanks [1], vacuum level control in chambers [2]. MEMS pressure sensors are pressure sensors fabricated with MEMS (Microelectromechanical Systems). Thanks to MEMS technology, MEMS pressure sensors have the advantages of small size, low cost, low energy consumption, and high resolution. MEMS pressure sensors have been widely used in many applications, such as automobiles, airplanes, submarines, biomedical devices, consumer products, etc. Various MEMS pressure sensors have been reported [3]-[11]. MEMS pressures sensor are fabricated with bulk-micromachining or surface-micromachining technologies. Among them, many MEMS pressure sensors are based on the deformation of a thin diaphragm. A vacuum cavity is sealed by a thin membrane. External pressure leads to the deformation of the thin diaphragm. Some piezoresistors are embedded around the diaphragm to form a Wheastone bridge. The deformation of the membrane induces stress (strains) inside the membrane, which leads to the resistance change of the embedded piezoresistors. Such tiny resistance change can be sensed by Wheastone bridge, and hence the applied pressure can be derived. In some other designs, the diaphragm forms parallel-plate capacitance with the substrate. The deformation of the diaphragm changes the capacitance gap between the diaphragm and the substrate. By measuring the capacitance change, the applied pressure change derived.

For some harsh environment, MEMS pressure sensors which can withstand high temperature or erosive chemicals are required [12]. For example, high temperature MEMS pressure sensors are needed in gas turbin engines, coal boilers, furnaces, and machinery for oil/gas exploration. For such high temperature applications, silicon material is not a good choice. Instead, some other alternative materials may be used, such as silicon carbide (SiC) [13][14], polycrystalline diamond [15] and ceramic materials [16]. Due to its high melting point (2730°C) and excellent thermal stability, silicon carbide (SiC) has become good candidate material for many MEMS high-temperature pressure sensors. Silicon carbide also has many other great properties, such as low density, high strength, low thermal expansion, high thermal conductivity, high hardness, high elastic modulus, excellent thermal shock resistance, superior chemical inertness. In this paper, a novel SiC based MEMS pressure sensor is proposed. The proposed MEMS pressure sensor utilizes the closed-loop operation of a SiC plate bonded inside the cavity between top Si diaphragm and bottom Si substrate. The SiC plate is supported by four folded SiC beams. When there is no external pressure, the SiC plate stays in the middle of the capacitance gap between top Si membrane and bottom Si substrate. When there is an external pressure, the top Si diaphragm deforms and hence the gap between SiC and top Si membrane is reduced. The MEMS pressure sensor utilizes electrostatic force to pull down the SiC membrane to maintain it in the middle position of the capacitance gap. The required driving voltage to keep the Si plate in the middle reflects the amount of deformation of the SiC plate, and in turn the value of the input pressure. The proposed SiC MEMS high temperature sensor does not need embedded piezoresistors, and can achieve high sensitivity due to the folded-beam structure and ultra-thin thickness of the Si diaphragm.

In this paper, a MEMS silicon carbide pressure sensor for high temperature application is proposed. This paper is arranged as below. The first section introduces the working principle of the pressure sensor. The theoretical model analysis of the pressure sensor is discussed in the second section. Some Matlab simulations are shown in the third section to show the relationship between displacement of the pressure sensor and its parameters, and a set of optimized design parameters for the pressure senor are derived. In the fourth section, ANSYS simulation is used to derive the vibrational modes of the pressure sensor. The fabrication flow of the proposed MEMS pressure sensor is suggested in the fifth section. Finally, some conclusions are drawn in the last section.

II. Device Design and Working Principle

The cross sectional view of the proposed SiC MEMS pressure sensor is shown in Figure 1. It has a silicon-SiC-silicon compound structure. A SiC round plate supported by four flexible folded beams is sealed inside a vacuum cavity between the top silicon diaphragm and bottom silicon substrate. Gold electrodes are deposited on the top and bottom surfaces of the SiC round plate, which constitute top and bottom capacitances with the top silicon diaphragm and bottom silicon substrate. When there is no external pressure, the SiC round plate stays in the middle of the gap, and the top capacitance equals to the bottom capacitance. If there is a non-zero external pressure, the top silicon diaphragm is pressed down so that the top capacitance gap is reduced, as shown in Figure 2(a). As a result, the top and bottom capacitance gaps are not equal any more. A control circuitry will sense this capacitance change, and a certain DC driving voltage is applied between the bottom gold electrode on the SiC plate and the silicon substrate, so that an electrostatic force is generated to pull down the SiC plate to the middle of the gap, as shown in Figure 2(b). In this way, the top capacitance is still equal to the bottom capacitance and the device works in a closed-loop mode. If the external pressure is large, the top silicon diaphragm deforms more, and a large driving voltage is required to pull the SiC plate back to the middle position of the gap. As a result, by measuring the required voltage to pull back the SiC plate, the value of the external pressure can be derived. This is the working principle of the MEMS pressure sensor.

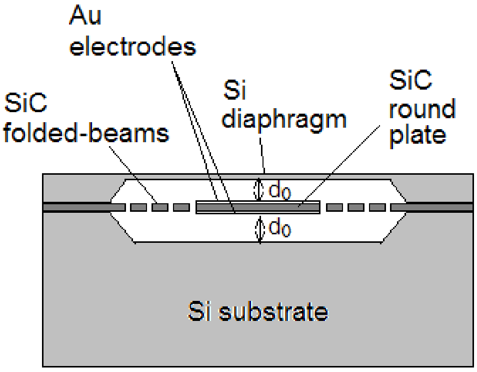

Figure 1. Cross sectional view of the designed SiC MEMS pressure sensor

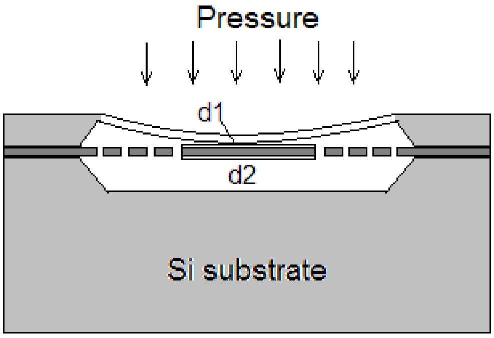

(a) Si diaphragm deforms under input pressure (The top and bottom capacitance gaps are not equal any more)

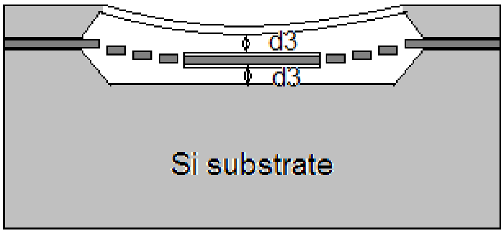

(b). Electrostatic force is used to pull down the SiC plate to maintain it in the middle position of the capacitance gap (so that top and bottom gap equals to each other with value of d3)

Figure 2. The working principle of the SiC MEMS pressure sensor

In order to improve the sensitivity of the pressure sensor, folded beam structure is used to support the SiC round plate, as shown in Figure 3.

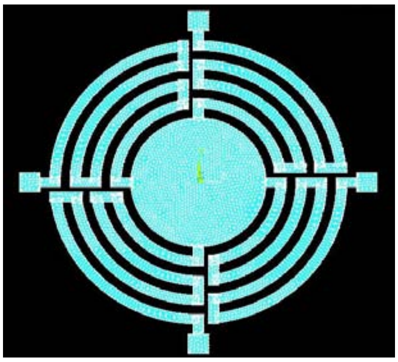

Figure 3. The designed SiC plate with four SiC folded beams

The proposed SiC MEMS pressure sensor utilized closed-loop operation of the SiC plate to sense the applied pressure. It eliminates the need for embedded piezoresistors, and can achieve high resolution due to the folded beam structure of the SiC sensing unit.

III. Performance Analysis of the MEMS Pressure Sensor

The SiC plate and its supported folded beams can be treated as simplified spring-mass model, as shown in Figure 4. In the closed mode, in order to pull down the SiC round plate to keep it in the middle position of the capacitance gap, electrostatic force *Fe* is applied to its surface toward substrate. The four beams deflect toward the substrate too, which leads to the vertical displacement of the SiC plate. Hence, it works in piston mode.

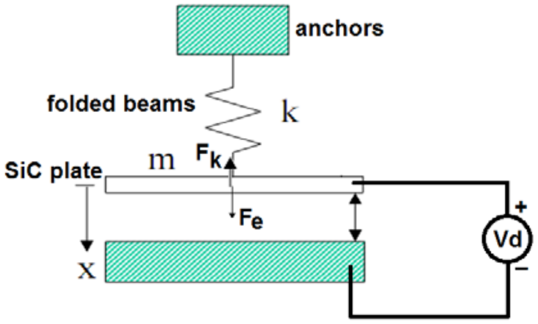

Figure 4. Spring-mass model of the SiC plate and the folded beams

Assume *m* is the mass of the plate, *Fe* is the electrostatic force on SiC plate due to driving voltage Vd, S_0 is the distance between the plate and the substrate, *x* is the displacement of the plate. When the electrostatic force balances the restoring force of the folded beams, $Fe=kx$, the SiC plate stays in its equilibrium position.

In the piston mode, the displacement of the SiC plate is caused by the deflection of the four SiC folded beams. Each folded beam has four sections connected in series, and each section can be treated as double-clamped beam model. Define the width and thickness of each folded beam as W_b and t_b separately. Assume the length of the four sections of a folded beam as W_{b1}, W_{b2}, W_{b3} and W_{b4} separately. As shown in Figure 3, the spring constants of the four sections of a folded beam can be calculated as below.

$$k_{b1}=\frac{Et_b w_b^3}{L_{b1}^3} \qquad k_{b2}=\frac{Et_b w_b^3}{L_{b2}^3} \qquad k_{b3}=\frac{Et_b w_b^3}{L_{b3}^3} \qquad k_{b4}=\frac{Et_b w_b^3}{L_{b4}^3} \tag{1}$$

Where E is the Young’s modulus of SiC material.
Each folded-beam has 4 sections in series, so the spring constant of each folded beam is

$$k_{fold}=\frac{1}{\frac{1}{k_{b1}}+\frac{1}{k_{b2}}+\frac{1}{k_{b3}}+\frac{1}{k_{b4}}} \tag{2}$$

The four folded-beams are in turn connected in parallel, so the total spring constant of the four folded beams is

$$k_{tot}=4k_{fold} \tag{3}$$

When there is no applied pressure, the SiC round plate stays in the middle of the capacitance gap, and the top and bottom capacitance gaps are both d0. In this way, top capacitance equals to bottom capacitance. When there is an applied pressure, the top Si diaphragm bends down for displacement of Δd. As a result, the top capacitance gap is changed to (d0-Δd), and the top capacitance does not equal to bottom capacitance any more. The control circuitry senses this capacitance change, and applies a driving voltage Vd between the SiC plate and the bottom Si substrate. As a result, an electrostatic force Fe is introduced to pull down the SiC plate by (Δd/2), so that it maintains the middle position again and the top and bottom between the new capacitance gap. The top and bottom capacitance gaps will equal to each other with the new value of (d0-Δd/2). The electrostatic force Fe should balance the restoring force of the folded beams as below.

$$F_e = \frac{\varepsilon S V_d^2}{2(d_0 - \frac{\Delta d}{2})^2} = K_{tot}\left(\frac{\Delta d}{2}\right) \tag{4}$$

Where ε is the dielectric constant of vacuum, S is the area of SiC round plate. Solving the above equation, the required driving voltage Vd to pull down the SiC round plate to the new middle position of the capacitance gap is

$$V_d = \sqrt{\frac{K_{tot} \cdot \Delta d}{\varepsilon S}} \cdot \left(d_0 - \frac{\Delta d}{2}\right) \tag{5}$$

By measuring the required driving voltage Vd, the resulted deformation Δd of the Si diaphragm due to input pressure can be derived, and hence the input pressure can be measured by considering the property of the Si diaphragm.

The deflection of the top Si diaphragm can be calculated using thin plate theory, in which the effects of both bending and stretching of the diaphragm are considered. Several assumptions are made [16]:

1). The edges of the diaphragm are clamped and can be modeled by built-in boundary conditions;
2). No residual stress is present in the diaphragm,
3). The diaphragms are subject to a uniform load.

Under above assumptions and large deflection theory for circular plate, the deformation d of a point with any radius *r* on the round Si diaphragm with radius *a* can be calculated by

$$d = d_0(1 - \frac{r^2}{a^2})^2 \tag{6}$$

Where d_0 is the maximum deflection at the center of the Si diaphragm, and d0 can be calculated by

$$\frac{d_0}{t} + 0.488(\frac{d_0}{t})^3 = \frac{3P(1-v^2)}{16E}(\frac{a}{t})^4 \tag{7}$$

Where t is the thickness of the Si diaphragm, and P is the applied pressure, ν is Poisson's ratio of Si material, and E is the Young's modulus of Si material. We can see that a larger pressure input will result in a larger maximum deformation of the Si diaphragm d0 in the center, which in turn requires larger driving voltage Vd to pull down the SiC round plate to the middle position of the new capacitance gap.

Based on above analysis, a set of optimized design parameters of the proposed SiC MEMS pressure sensor are obtained, as shown in Table 1.

Table 1. Optimized design parameters of the MEMS pressure sensor

Design Parameters	Values
Radius of SiC round Plate (a)	40 μm
Thickness of SiC plate (t)	1 μm
Fold beam radius of 1st section (r_1)	50 μm
Folded beam radius of 2nd section (r_2)	60 μm
Folded beam radius of 3rd section (r_3)	70 μm
Folded beam radius of 4th section (r_4)	80 μm
Folded beam length of 1st section (L_{b1})	70 μm
Folded beam length of 2nd section (L_{b2})	84 μm
Folded beam length of 3rd section (L_{b3})	98 μm
Folded beam length of 4th section (L_{b4})	112 μm
Static gap between SiC plate and substrate (d_0)	12 μm

Based on hand calculation using the previous theoretical analysis, the expected performance parameters of the designed MEMS pressure sensor are shown in Table 2.

Table 2. Performance parameters of the MEMS pressure sensor

Performance	Values
SiC plate mass	1.56×10^{-11} kg
Spring constant of the four folded beams	153.06 N/m
Resonant frequency (hand calculation)	149860 Hz
Resonant frequency(ANSYS simulation)	175450 Hz

IV. ANSYS Simulation

Resonant frequency, which is a natural frequency of vibration determined by the physical parameters of the vibrating object, is an important characteristic for the proposed pressure sensor. In order for fast response, we would prefer a larger resonant frequency of the SiC round plate. However, this means a larger spring constant, and in turn requires larger driving voltage to pull down the SiC plate to middle position. Thus there is a trade-off in the design. Furthermore, the resonant frequency of the working mode needs to be separated far away from its neighborhood vibration modes to avoid interference and ensure stability during its working mode. ANSYS FEM simulation is used to simulate the first five vibration modes of the proposed MEMS pressure sensor, and the corresponding resonant frequencies are extracted. For the above MEMS pressure sensor design, the ANSYS modal simulation results are listed as below.

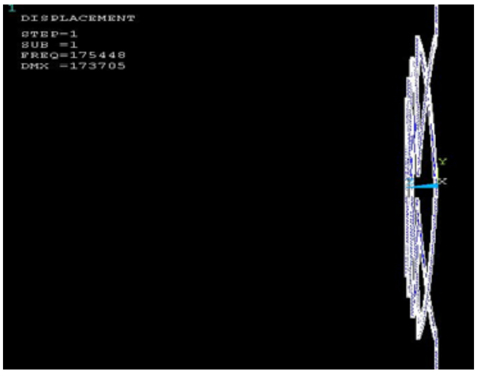

Figure 5. ANSYS simulation result of vibration mode #1: The SiC plate moves up and down, perpendicular to the substrate surface (resonant frequency: f1=175450 Hz)

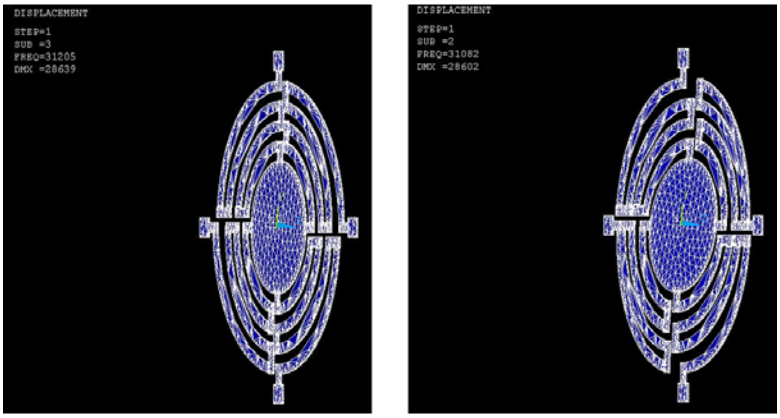

(a) Vibration mode #2 (b). Vibration mode #3

Figure 6. ANSYS simulation results of vibration mode #2 and #3: The SiC plate rotates, with resonant frequencies of 31082 Hz and 31206 Hz separately.

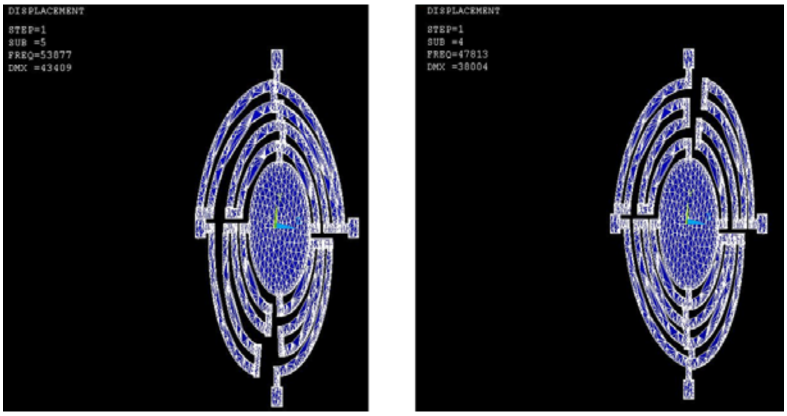

(a) Vibration mode #4 (b). Vibration mode #5

Figure 7. ANSYS simulation results of vibration mode #4 and #5: The SiC plate bends, with resonant frequencies of 47814Hz and 53878 Hz separately.

Based on above simulations, the working mode of the pressure sensor is mode #1 (SiC plate moves up and down perpendicular to the substrate surface), and the resonant frequency is 17545 Hz. Furthermore, ANSYS simulation is also used to find out the displacement of the SiC plate under giving certain electrostatic force. The results are shown as below.

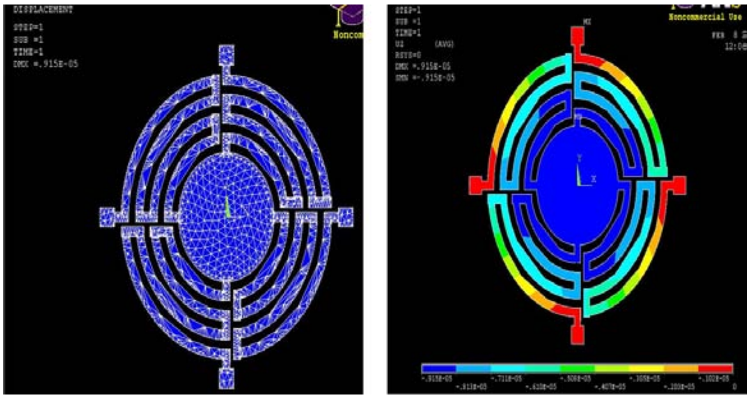

Figure 8. ANSYS simulation results of the SiC plate under certain electrostatic force (the maximum displacement is 9.152μm)

VI. Conclusion and Future Work

In this paper, the design and simulation of a novel SiC MEMS pressure sensor is proposed. The working principle of the MEMS pressure sensor is analyzed. ANSYS FEM simulation is used to simulate the first five vibration modes of the sensor, and the corresponding resonant frequencies are extracted. The resonant frequency of the proposed MEMS pressure sensor is found to be 175450Hz. Based on the simulation, a set of optimized design parameters are suggested. The corresponding performance parameters are also listed. The proposed pressure sensor can be used for pressure monitoring in high temperature applications, such as oil storage tanks, vacuum level control in chambers, gas turbine engines and oil wells. In the future work, we will design the signal control circuitry for the closed-loop operation of the MEMS pressure sensor.

References

[1] A. Wang, et al., "Optical fiber pressure sensor based on photoelastic effect and its applications," *Journal of Lightwave Technology*, 10, pp. 1466-1472, 1992.

[2] B. C. S. Chou, J.-S. Shic, and Y.-M. Chen. "A highly sensitive pirani vacuum gauge," *The 8th International Conference on Solid-State Sensors and Actuators: Eurosensors IX. Transducers'95*, Vol. 2, pp. 167-170, 1995.

[3] W. P. Eaton and J. H. Smith, “Micromachined pressure sensors: Review and recent developments” *Proc. SPIE - The International Society for Optical Engineering*, Vol. 3046, pp. 30-41, 1997.

[4] G. Blasquez, P. Pons, and A. Boukabache, “Capabilities and limits of silicon pressure sensors,” *Sensors and Actuators A: Physical*, Vol. 17, pp. 387-403, 1989.

[5] W. H. Ko, “Solid-state capacitive pressure transducers,” *Sensors and Actuators A: Physical*, Vol. 10, pp. 303-320, 1986.

[6] K. Suzuki, S. Suwazono, and T. Ishihara, “Integrated silicon pressure sensor,” *IEEE J. Solid-State Circuits*, Vol. SSC-22, pp. 151-156, 1987.

[7] J. T. Kung and H. -S. Lee, “An integrated air-gap-capacitor pressure sensor and digital readout with sub-100 attofarad resolution,” *IEEE J. Microelectromechanical Systems*, Vol. 1, pp. 121-129, 1992.

[8] S. K. Clark and K. D. Wise, “Pressure sensitivity in anisotropically etched thin-diaphragm pressure sensors,” *IEEE Trans. Electron Devices*, Vol. ED-26, pp. 1887-1896, 1979.

[9] C. H. Mastrangelo, X. Zhang, and W. C. Tang, “Surface-micromachine capacitive differential pressure sensor with lithographically defined silicon diaphragm,” IEEE Journal of Microelectromechanical Systems, Vol. 5, pp. 89-105, 1996.

[10] H.Guckel, “Surface micromachined pressure transducers,” *Sensors and Actuators A: Physical*, Vol. A28, pp. 133-146, 1991.

[11] S. Sugiyama, K. Shimaoka, and O. Tabata, “Surface micromachined micro-diaphragm pressure sensors,” *Proc. 6th Int. Conf. Solid-State Sensors and Actuators (Transducers’91)*, pp. 188-191, 1991.

[12] B. Qi, et al. "Fiber optical pressure and temperature sensors for oil down hole applications," *Proceedings of SPIE*, Vol, 4578. pp. 182-190, 2002.

[13] A.A. Ned, et al. "Dynamic pressure measurements using silicon carbide transducers," *Instrumentation in Aerospace Simulation Facilities, 9th International Congress on ICIASF*, pp. 240-245, 2001.

[14] R. Okojie, A. Ned, D. Kurtz, and W. Carr, “6H-SiC pressure sensor for high temperature applications,” *Proc. 1996 IEEE/ASME MEMS Workshop*, pp. 146-149, 1996.

[15] E. Obermeier, “High temperature microsensors based on polycrystalline diamond thin films,” *Proc. 8th International Conference on Solid State Sensors and Actuators (Transducers’95*), Vol. 2, pp. 178-181, 1995.

[16] M.A. Fonseca, J.M. English, M. Arx, and M.G. Allen, “Wireless Micromachined Ceramic Pressure Sensor for High-Temperature Applications”, *IEEE Journal of Microelectromechanical Systems*, Vol. 11, No. 4, Aug. 2002.